USING AN OCEANIC ACOUSTIC NOISE MODEL TO EVALUATE SIMULATED ATMOSPHERIC STATES

P. Letournel [1,2], C. Listowski [1], M. Bocquet [2], A . Le Pichon [1], A. Farchi [2]

[1] CEA, DAM, DIF, F-91297, Arpajon, France. [2] CEREA (Atmospheric Environment Center), Joint Laboratory École des Ponts ParisTech and EDF R&D, Université Paris-Est, 77455 Marne-la-Vallée, France

Introduction

Infrasound are low frequency (below 20 Hz) acoustic waves which propagate through the atmosphere up to thousands of kilometers due to their weak attenuation and thanks to waveguides established between the surface and the middle atmosphere (MA, 10-90 km). Infrasound sources can be anthropogenic (explosions, wind farms…) or natural (volcanoes, ocean waves…). Infrasound waves are continuously monitored over the globe by a network of 53 certified infrasound stations (over the 60 planned) installed to ensure compliance with the Comprehensive Nuclear Test Ban Treaty (CTBT). They are part of the international monitoring system (IMS). **Ocean waves interactions contribute to a large extent to the worldwide coherent acoustic noise between 0.1 and 0.6 Hz**. The atmospheric infrasound by ocean waves (ARROW) model *[1] [2]* developed by CEA and IFREMER, simulate oceanic infrasound emissions (called microbaroms) using the ocean wave model WAVEWATCH III®. Infrasound propagation dependency on the middle atmospheric waveguides suggests that microbarom observations can informs on the state of the MA. As **numerical weather prediction (NWP) models are poorly constrained in the MA**, due to a lack of observations, **microbaroms detections appear as a unique source of global and continuous observations, which could serve to enhance the prediction capability of NWP models in the MA.** This would also benefit surface weather predictions because of the influence of the MA on surface meteorology at subseasonal-to-seasonal scales *[3]*.

IMS Infrasound stations

Each of the 53 certified station is composed of several sensors a few km apart. **Array processing allows to estimate parameters (Azimuth, Trace velocity, Amplitude…)** of coherent infrasound wavefronts crossing the station at a given time/frequency.

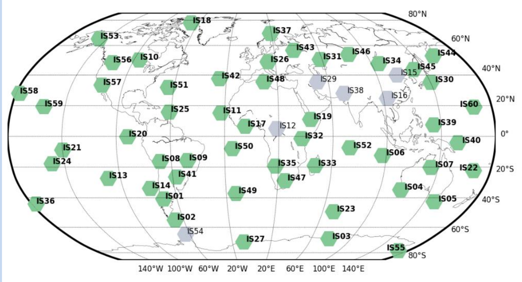

International Monitoring System (IMS) infrasound stations. Green: certified Grey: planned

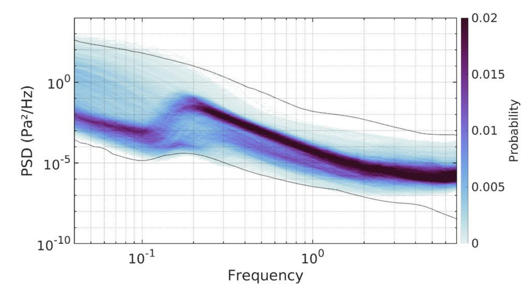

Power Spectrum Density (PSD) at IS37. The microbarom emission peak is centered around 0.2 Hz.

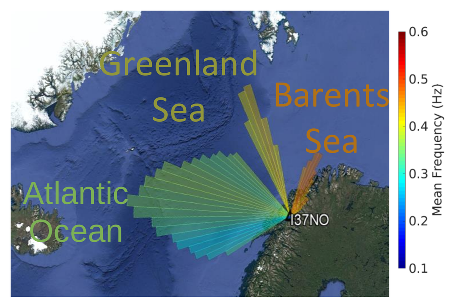

Polar histogram of microbaroms detections for the station IS37. Color codes the frequency associated to detections.

Infrasound propagation

Infrasound propagate over thousands of km through atmospheric waveguides. The existence of a guide in the direction of propagation is conditioned by the effective sound speed $c_{eff} = c_{sound} + \vec{v}_{wind}.\vec{n}$ with c_{sound} the adiabatic sound speed, $\vec{v}_{wind}$ the wind speed, $\vec{n}$ the unit vector normal to the wavefront.

In the geometric acoustics approximation, if $C_{ratio} = \frac{c_{eff}(z)}{c_{eff\,(source)}} > 1$, then a waveguide is present at altitude z.

Updating MCML detection algorithm for microbaroms

We adapt the Multichannel Maximum-Likelihood (MCML) algorithm developed at CEA (Poste et al. 2022 [4]), to detect mircrobaroms between 0 and 360° azimuth.

MCML estimates the direction of arrival (θ), trace velocity (v), signal amplitude (s) and noise amplitude (σ) through a likelihood maximization on a (θ, v) grid.

Instead of classically estimating s for the couple $(\hat{\theta}, \hat{v})$ maximizing the likelihood, the maximization of the likelihood with respect to s is explicitly solved for each couple (θ, v) of the grid.

We average estimated signal amplitudes for trace velocities from 340 to 380 m/s and normalize to obtain an observed azimuthal distribution of amplitude.

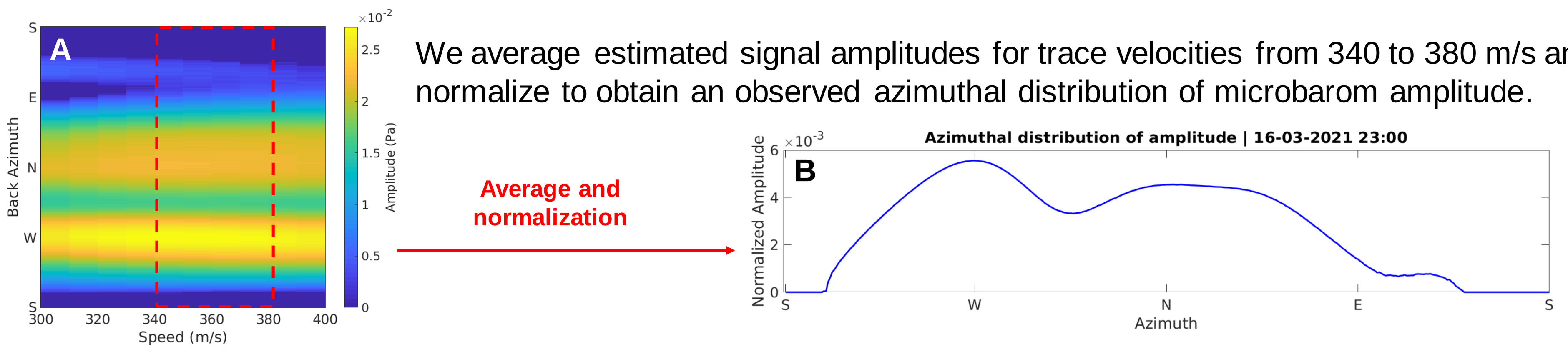

(**A**) Estimation of the signal amplitude s on a (θ, v) grid using the MCML algorithm for 1 hour of infrasound signal from IS37 in March 2021.
(**B**) Corresponding azimuthal distribution of microbarom amplitude after integration and normalization.

The microbarom source model: ARROW

The microbarom source model is based on the Hasselmann integral $H(f_s)$ which describes oceanic waves interaction and is computed by WAVEWHATCH III® (WW3). The **acoustic intensity (W.m^{-2}.Hz^{-1}) is derived** using a multiplicative acoustic factor F_{ac} *[1] [2]* .

Grids of 0.5° x 0.5° lat/lon spatial resolution with a 3h temporal resolution, for frequencies from 0.08 to 0.6 Hz are remapped to circular grids centered on the infrasound station.

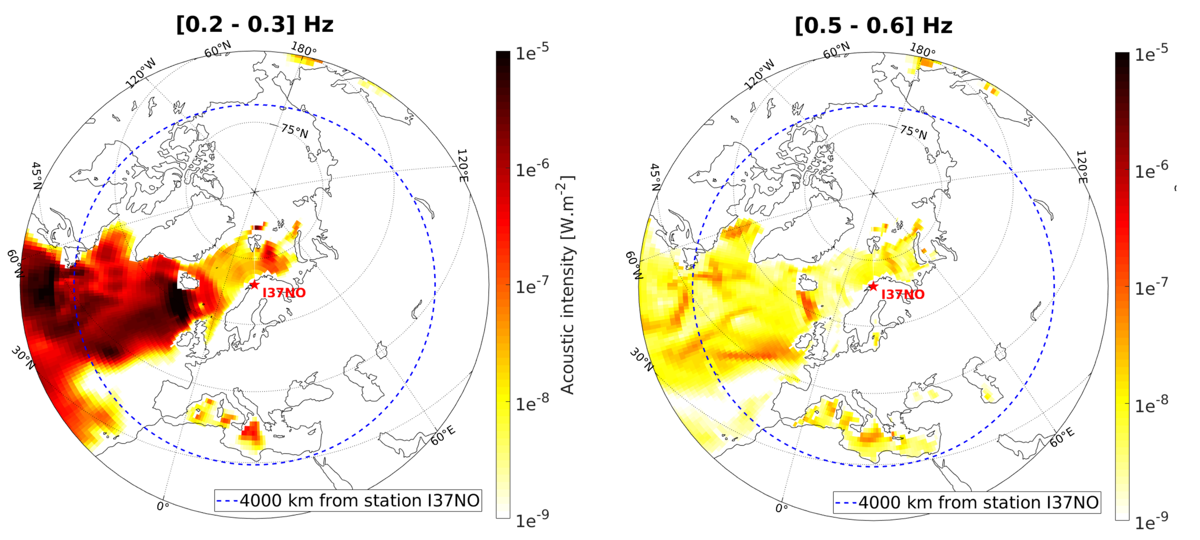

Spatial and frequency dependency of the microbarom model remapped in a circular grid with 1° azimuthal resolution around IS37.

Evaluating NWP models and sensitivity to propagation methods

We simulate infrasound propagation with two methods:

- A **semi-empirical attenuation law** (updated version from Le Pichon et al . (2012) [5]) using atmospheric wind and temperature profiles above the stationof interest.
- More realistic **Parabolic Equation (PE)** range-dependant propagation [6] prescribing the full 3D atmospheric fields

We compare two Numerical Weather Prediction models:

- **WACCM** (NCAR's forecast product, version 6, up to ~130 km)
- **ERA5** (ECMWF's re-analysis, cy41r2, up to ~80 km) + HWM-14/NRLMSISE-00 (up to ~130 km)

Attenuation and microbaroms source map are combined and processed to obtain simulated **azimuthal distributions of amplitude**. The **array response** is also taken into account. We assess NWP model performance and sensitivity to the progation method through comparisons between simulated and observed distributions.

We use a circular optimal transport metric: the **circular Wasserstein distance** ($\in [0{:}\,0.5]$), the lower the better [7], [8].

Effect of the propagation method | **Effect of atmospheric specification using PE**

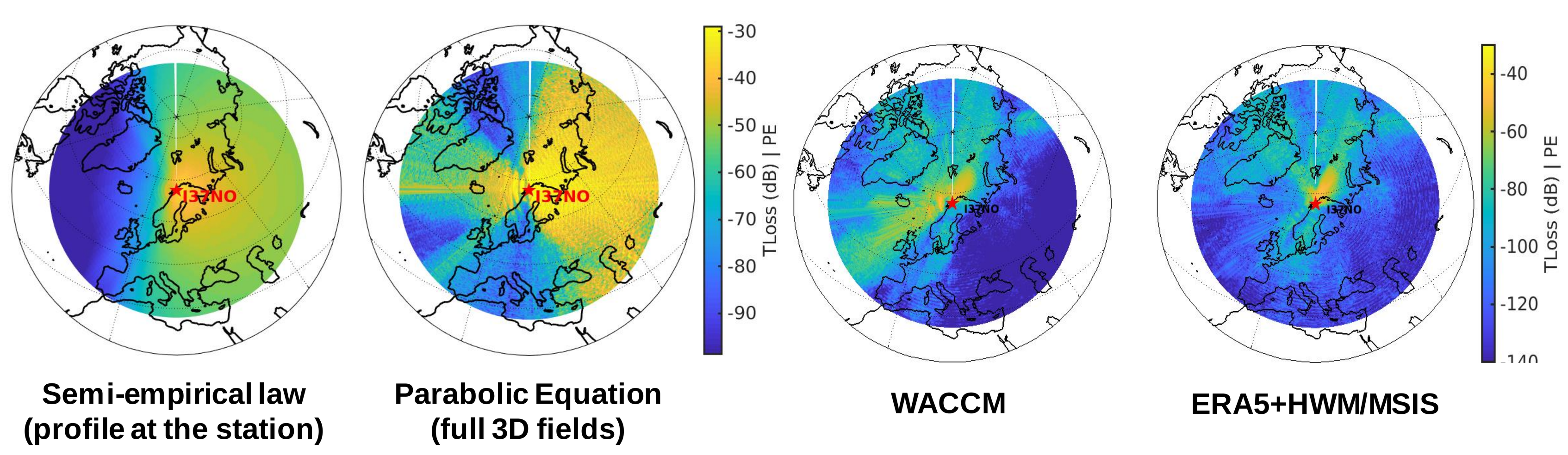

Attenuation maps illustrating differences induced by the propagation method (left) or the atmospheric specifications (right). These figures illustrate the need to account for the full 3D atmospheric fields.

Results

Yearly simulated and observed microbaroms

(A) modeled azimuthal distribution of microbaroms amplitude with WACCM atmospheric specifications and PE propagation every six hour over 2021. (B) Observed azimuthal distribution of microbaroms amplitude every hour over 2021.

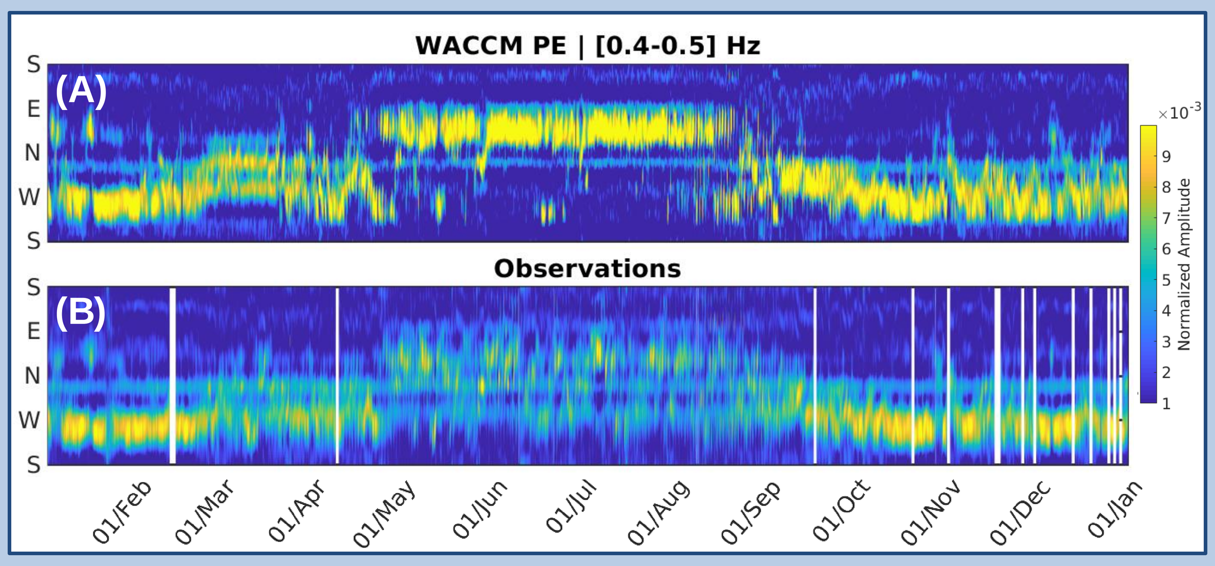

- The strong stratospheric waveguide created by the polar vortex in summer leads to observations of microbaroms moslty from the West (Atlantic Ocean) during the winter.
- We reproduce the sidelobes from the array/algorithm response in simulations (see N-N-W and S-E for instance).
- Simulations overestimate the inversions of the main directions of arrival (two inversion in January due to a SSW and globally degraded performances in summer).

Thermospheric microbarom arrivals

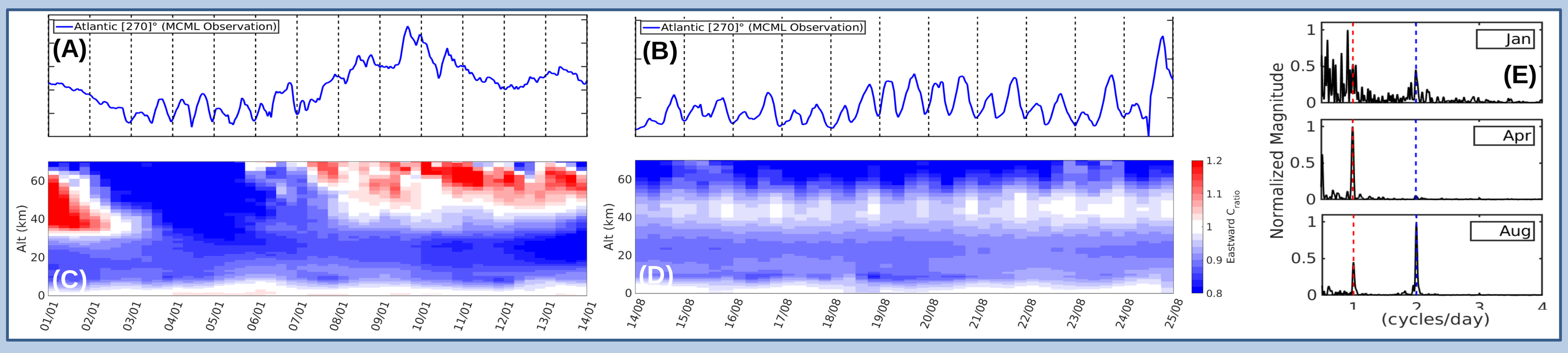

(A) and (B) Observed microbaroms amplitude coming from the Atlantic Ocean (270°) for part of January and August respectively. (C) and (D) associated atmospheric conditions eastward propagation over 4000 km to IS37, represented by the average C_{ratio} as a function of altitude. (E) PSD of the observed amplitude from the Atlantic Ocean (270°), for January, April, and August 2021.

- Observed semi-diurnal oscillations in the absence of a strong stratospheric waveguide : mainly in summer and during the January 2021 Sudden Stratospheric Warming.
- Observed semi-diurnal oscillations are evidences of Mesosphere and Lower Thermosphere (MLT) infrasound propagation because of the semi-diurnal tides at these altitudes.
- Need to account for the MLT in simulated atmospheric propagation.

Sensitivity to the propagation method

- Yearly simulations were carried out to evaluate our ability to assess NWP models performances using the semi-empirical law.
- Differences between simulated distributions using different NWP models are much to smaller when propagating. with the semi-empirical law.
- Inter-model differences are better rendered when using the PE method.

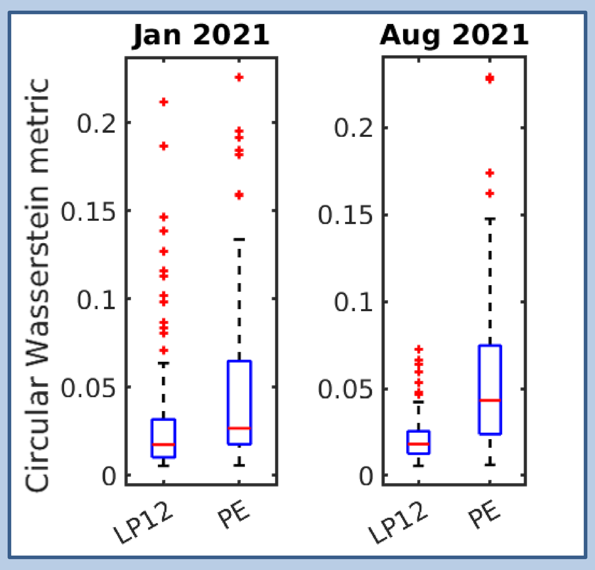

Circular Wasserstein metric between simulated distribution using WACCM and ERA5+HWM/MSIS atmospheric specification, for January and August 2021. For each month, the left boxplot is associated with simulations using the semi-empirical law while the right one is associated with PE simulations.

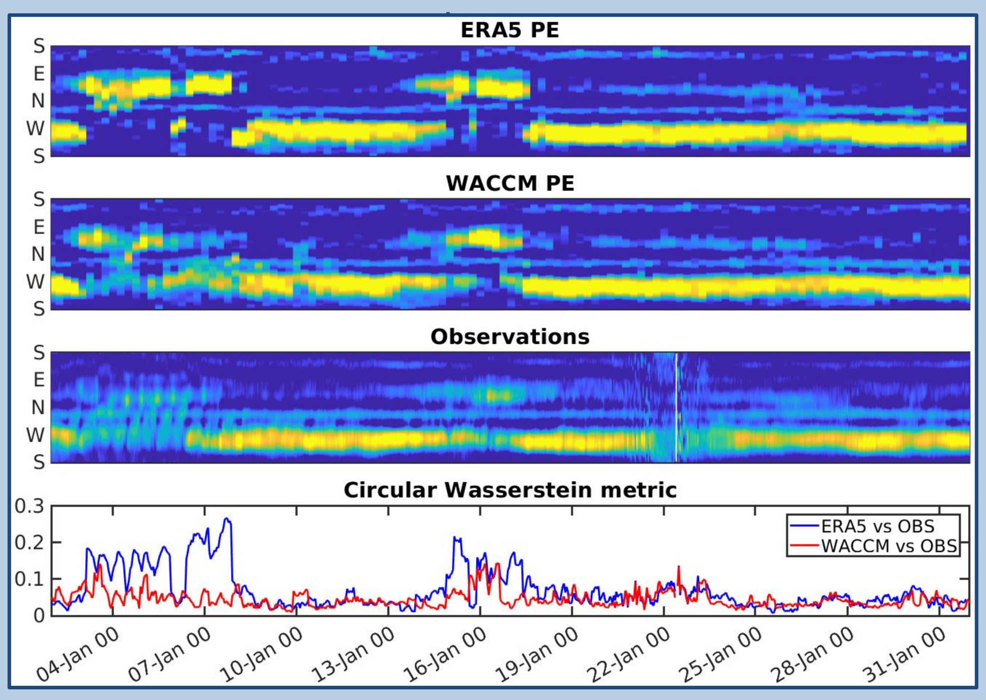

(A) and (B) PE simulations using respectively ERA5+HWM/MSIS and WACCM atmospheric specifications, over January 2021. (C) MCML observations for the corresponding month. (D) Wassertstein metric between (A) and (C) (in blue) and between (B) and (C) (in red).

NWP models assessment and conclusions

- In the winter, the stratospheric polar vortex induces a strong eastward waveguide. The vortex is perturbated twice in January during the Sudden Stratospheric Warming.
- WACCM better reproduces the observed bimodality of distributions during the SSW.
- The metric can be used to summarizes the two models NWP relative performances.

Perspectives: the present conclusions will guide the developpement of a framework for assimilating microbaroms observations in atmospheric models.

References

[1] De Carlo et al. (2020), Geophysical Journal International, 221(1), 569–585.
[2] De Carlo et al. (2022), EGU General Assembly 2022, Vienna, Austria, 23–27 May 2022, EGU22-7564.
[3] Domeisen et al. (2020), Journal of Geophysical Research Atmospheres. 125.
[4] Poste et al. (2022), Geophysical Journal International, Volume 232, Issue 2, February 2023, Pages 1099–1112.
[5] Le Pichon et al. (2012), J. Geophys. Res.-Atmos., 117, 1–12
[6] Waxler et al. (2017), The Journal of the Acoustical Society of America, 141(5_Supplement), 3627-3627.
[7] Hundrieseret al. (2022), In *Directional Statistics for Innovative Applications: A Bicentennial Tribute to Florence Nightingale* (pp. 57-82). Singapore: Springer Nature Singapore.
[8] Flamary et al. (2021). Journal of Machine Learning Research, 22(78), 1-8.